ISSCR

OPEN ACCESS

ICAM-1 Deficiency in the Bone Marrow Niche Impairs Quiescence and Repopulation of Hematopoietic Stem Cells

Yu-feng Liu,[1,3,9,10] Shao-ying Zhang,[2,3,10] Ying-ying Chen,[3] Kun Shi,[4] Bin Zou,[5] Jun Liu,[3] Qiong Yang,[3] Hua Jiang,[4] Lai Wei,[5] Chang-zheng Li,[6] Meng Zhao,[6] Dmitry I. Gabrilovich,[3,7,8] Hui Zhang,[3,7,*] and Jie Zhou[1,3,7,*]

[1]Key Laboratory of Immunology, Sino-French Hoffmann Institute, School of Basic Medical Sciences, Guangzhou Medical University, Guangzhou 511436, China
[2]National & Local Joint Engineering Research Center of Biodiagnosis and Biotherapy, The Second Affiliated Hospital, Xi'an Jiaotong University, Xian 710000, China
[3]Institute of Human Virology, Zhongshan School of Medicine, Sun Yat-sen University, Guangzhou 510080, China
[4]Guangzhou Women and Children's Medical Center, Guangzhou 510000, China
[5]Zhongshan Ophthalmic Center, Sun Yat-sen University, Guangzhou 510060, China
[6]Key Laboratory for Stem Cells and Tissue Engineering, Sun Yat-sen University, Guangzhou 510080, China
[7]Key Laboratory of Tropical Disease Control, Chinese Ministry of Education, Sun Yat-sen University, Guangzhou 510080, China
[8]The Wistar Institute, Philadelphia, PA 19104, USA
[9]Guangdong Provincial Key Laboratory of Allergy & Clinical Immunology, The Second Affiliated Hospital, Guangzhou Medical University, Guangzhou 511436, China
[10]Co-first author
*Correspondence: zhangh92@mail.sysu.edu.cn (H.Z.), zhouj72@mail.sysu.edu.cn (J.Z.)
https://doi.org/10.1016/j.stemcr.2018.05.016

SUMMARY

The bone marrow niche plays a critical role in controlling the fate of hematopoietic stem cells (HSCs) by integrating intrinsic and extrinsic signals. However, the molecular events in the HSC niche remain to be investigated. Here, we report that intercellular adhesion molecule-1 (ICAM-1) maintains HSC quiescence and repopulation capacity in the niche. ICAM-1-deficient mice (ICAM-1$^{-/-}$) displayed significant expansion of phenotypic long-term HSCs with impaired quiescence, as well as favoring myeloid cell expansion. ICAM-1-deficient HSCs presented normal reconstitution capacity during serial transplantation; however, reciprocal transplantation experiments showed that ICAM-1 deficiency in the niche impaired HSC quiescence and repopulation capacity. In addition, ICAM-1 deletion caused failure to retain HSCs in the bone marrow and changed the expression profile of stroma cell-derived factors, possibly representing the mechanism for defective HSCs in ICAM-1$^{-/-}$ mice. Collectively, these observations identify ICAM-1 as a regulator in the bone marrow niche.

INTRODUCTION

Hematopoiesis is the process whereby the pool of all mature blood cells is replenished throughout an organism's life time (Doulatov et al., 2012; Sawai et al., 2016). Hematopoietic stem cells (HSCs) have the capability of both self-renewal and differentiation, which ensures their homeostasis and maintains the hematopoietic system (Orford and Scadden, 2008). Under steady-state conditions, HSCs reside in a dormant state characterized by slow cell cycling, such as quiescence or G0 phase (Pietras et al., 2011). In response to stress, injury, or infections, HSCs exit the G0 phase and proliferate to generate hematopoietic progenitor cells, which will subsequently differentiate and reconstitute the blood and immune lineages (Nakamura-Ishizu et al., 2014; Wilson et al., 2008, 2009). The bone marrow microenvironment, which is known as the niche, has been shown to play a major role in the precise equilibrium between quiescence, self-renewal, and differentiation of HSCs (Crane et al., 2017; Schofield, 1978). The bone marrow niche contains a variety of stroma cells types that help maintain HSC function by providing

extracellular matrix proteins, cytokines, chemokines, and growth factors (Mendelson and Frenette, 2014). Stroma cells can interplay with HSCs in the niche, either by secreting certain factors or via direct cell-cell communication through signaling molecules expressed on the cell surface; in this way, they are uniquely adapted to support HSCs (Blaser et al., 2017; Greenbaum et al., 2013; Suda et al., 2005).

The cellular and molecular mechanisms regulating the interplay between HSCs and the bone marrow niche have been extensively investigated (Arai et al., 2004; Goncalves et al., 2016). Among these, adhesion molecules play an important role not only in terms of anchoring hematopoietic cells to the bone marrow niche but also by regulating their functional status (Chen et al., 2013; Jeannet et al., 2013; Simmons et al., 1997). HSCs express diverse adhesion receptors, such as P selectin glycoprotein ligand-1 (PSGL-1), integrins α4β1 and α5β1, and very late antigen-4 (VLA-4), which interact with extracellular matrix proteins and cell adhesion molecules expressed by niche cells (Prosper and Verfaillie, 2001; Winkler et al., 2012). In addition to retaining HSCs in the proper bone marrow niche, the interaction
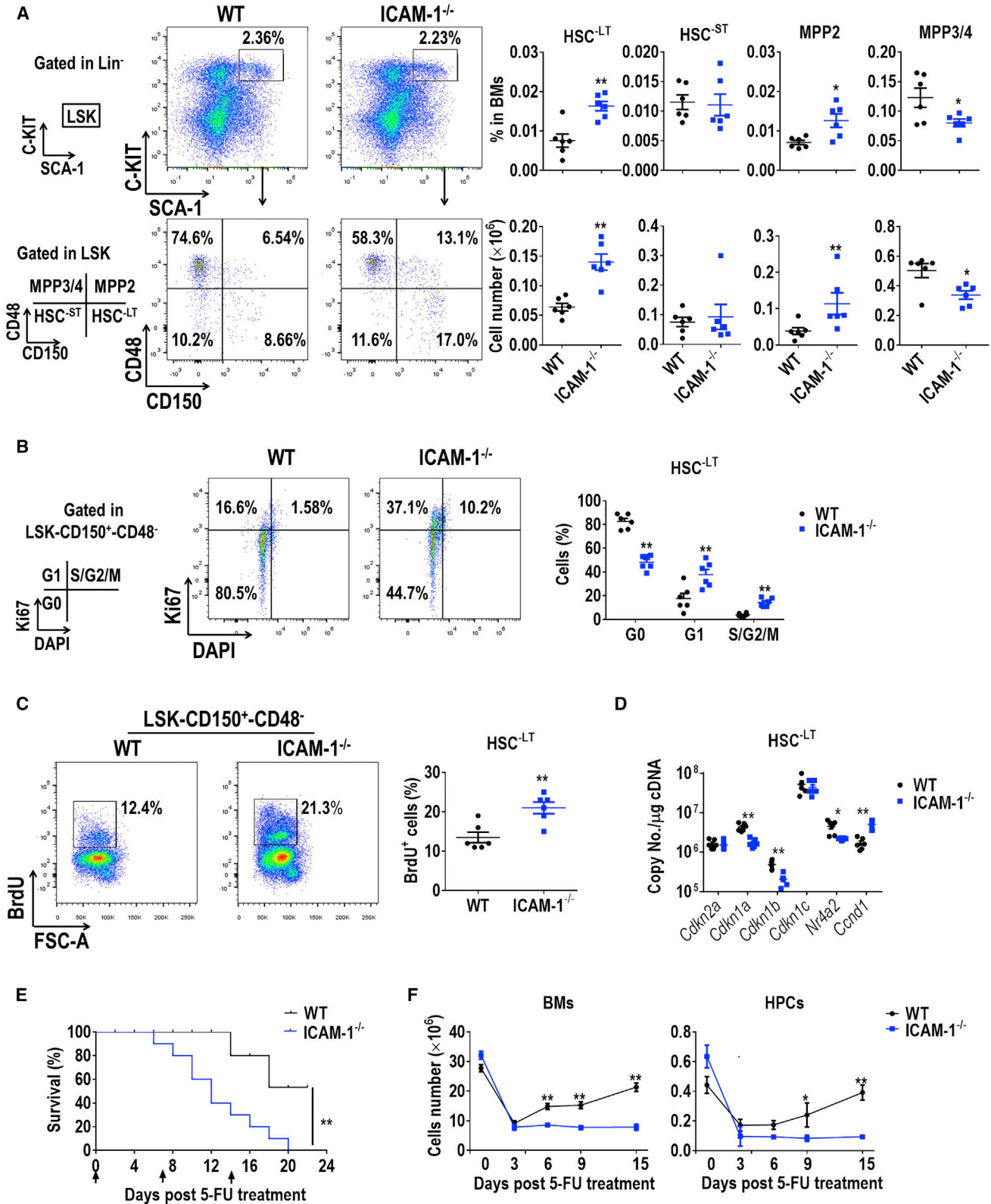
(legend on next page)

between adhesion receptors and their ligands could elicit intracellular signaling in HSCs and thus regulate their functionality (Papayannopoulou et al., 1995; Papayannopoulou and Nakamoto, 1993; Vermeulen et al., 1998; Wilson and Trumpp, 2006).

Intercellular adhesion molecule-1 (ICAM-1) is a member of the immunoglobulin superfamily of adhesion proteins, which share a similar structure of repeating immunoglobulin-like domains (van de Stolpe and van der Saag, 1996). Upon binding to its ligand β_2 integrin, lymphocyte function-associated antigen-1 (LFA-1), ICAM-1 mediates cellular cross-talk, including among immune cells (Carrasco et al., 2004). Their interaction enables leukocyte trafficking and activation, the formation of the immunological synapse between T cells and antigen-presenting cells, as well as establishment of memory T cells (Boyd et al., 1988; Long, 2011; Scholer et al., 2008). In contrast to its broad effect on the functionality of immune cells, the role of ICAM-1 in HSCs and hematopoiesis remains largely unknown. Treatment of human CD34+ cells with anti-LFA-1 antibody was reported to significantly reduce HSCs engraftment (Peled et al., 2000). These observations indicated a potential role of ICAM-1 and LFA-1 in the regulation of HSC biological functions.

In this study, we investigated the regulatory effect of ICAM-1 in HSCs. We show that ICAM-1 is an important regulator of HSC homeostasis, which acts in a niche-dependent manner. Deficiency of ICAM-1 in mice resulted in expansion of phenotypic long-term HSCs (HSC^{-LT}) with defective quiescence and repopulation capability. Either the progenitor or progeny cells exhibited an increase in the myeloid lineage, and a decrease in the lymphoid lineage. Moreover, these effects were mediated by the bone marrow niche rather than being intrinsic to HSCs. ICAM-1 deficiency in the bone marrow niche results in dysregulation of stroma cell-derived factors, which may also underlie the potential mechanism of action of the niche. Taken together, our results reveal ICAM-1 as a regulator of HSCs in the bone marrow niche.

RESULTS

ICAM-1 Deficiency Causes Expansion of HSC^{-LT} with Impaired Quiescence

To address the role of ICAM-1 in HSCs under steady-state conditions, we evaluated the levels of hematopoietic stem and progenitor cells (HSPCs) in the bone marrow from ICAM-1-deficient (ICAM-1$^{-/-}$) mice and wild-type (WT) littermate controls. Flow cytometric analysis showed that ablation of ICAM-1 caused a minor increase in bone marrow cellularity (Figure S1A), whereas the frequency of Lin$^-$ SCA-1$^+$ C-KIT$^+$ (LSK) did not differ statistically between ICAM-1$^{-/-}$ and WT mice (Figure S1B). However, the proportion and absolute cell counts of long-term HSCs (HSC^{-LT}, LSK-CD150$^+$CD48$^-$) in the bone marrow were more than 2-fold higher upon ICAM-1 deletion (Figure 1A). Instead, no noticeable changes were detected for short-term HSC (HSC^{-ST}, LSK-CD150$^-$CD48$^-$) cells (Figure 1A). Additionally, the level of multipotent progenitor (MPP) 2 (LSK-CD150$^+$CD48$^+$) was significantly elevated, whereas the MPP3/4 (LSK-CD150$^-$CD48$^+$) subset was reduced following ICAM-1 deletion (Figure 1A). The expansion of HSC^{-LT} was further confirmed by staining with another set of HSCs markers, CD34 and FLK2. These helped to distinguish the HSC^{-LT} (LSK-CD34$^-$FLK2$^-$), HSC^{-ST} (LSK-CD34$^+$FLK2$^-$), MPP (LSK-CD34$^+$FLK2$^+$) cell population, and confirmed a roughly 2-fold increase in HSC^{-LT} (Figure S1C). The above observations prompted us to investigate the cycling status of HSC^{-LT}. Ki67 staining showed a significant reduction in G0 cells (Ki67$^-$DAPI$^-$, 79.2% ± 10.56% in WT versus 48.2% ± 5.56% in ICAM-1$^{-/-}$) and increase in cycling cells (S/G2/M; Ki67$^+$DAPI$^+$, 3.58% ± 1.47% in WT versus 14.12% ± 3.14% in ICAM-1$^{-/-}$) in ICAM-1-deficient HSC^{-LT} compared with WT controls (Figure 1B). Another cell-cycle staining method, Pyronin Y/Hoechst, produced the same results (Figure S1D). Furthermore, pulse bromodeoxyuridine (BrdU) labeling identified a higher proportion of proliferating cells in ICAM-1-deficient HSC^{-LT} (13.5% ± 3.27% in WT versus 21.0% ± 3.57% in ICAM-1$^{-/-}$) (Figure 1C). Consistent with its

Figure 1. ICAM-1 Deficiency Causes Expansion of HSC^{-LT} with Impaired Quiescence
(A) Flow cytometric analysis of HSPCs in bone marrow from WT and ICAM-1$^{-/-}$ mice. HSC^{-LT}, long-term HSCs; HSC^{-ST}, short-term HSCs; MPPs, multipotent progenitors.
(B) Cell-cycle analysis of HSC^{-LT} (LSK-CD48$^-$CD150$^+$) from WT and ICAM-1$^{-/-}$ mice.
(C) BrdU incorporation analysis of HSC^{-LT} from WT and ICAM-1$^{-/-}$ mice. In (A)–(C), representative profiles are shown at left, and the proportion and absolute cell numbers are shown at right. Data are shown as the mean ± SEMs from three independent experiments (n = 6).
(D) The expression of cell cycle-related genes in HSC^{-LT} was examined by absolute quantification real-time PCR. Data are shown as the mean ± SEMs from three independent experiments (n = 6).
(E) Survival curve of WT or ICAM-1$^{-/-}$ mice following weekly 5-FU treatment (150 mg/kg body weight) (n = 12).
(F) Dynamic changes of bone marrow cell numbers (left) and HPCs numbers (right) in WT and ICAM-1$^{-/-}$ mice during 5-FU challenge. Mean ± SEMs from six mice are shown.
*p < 0.05; **p < 0.01.
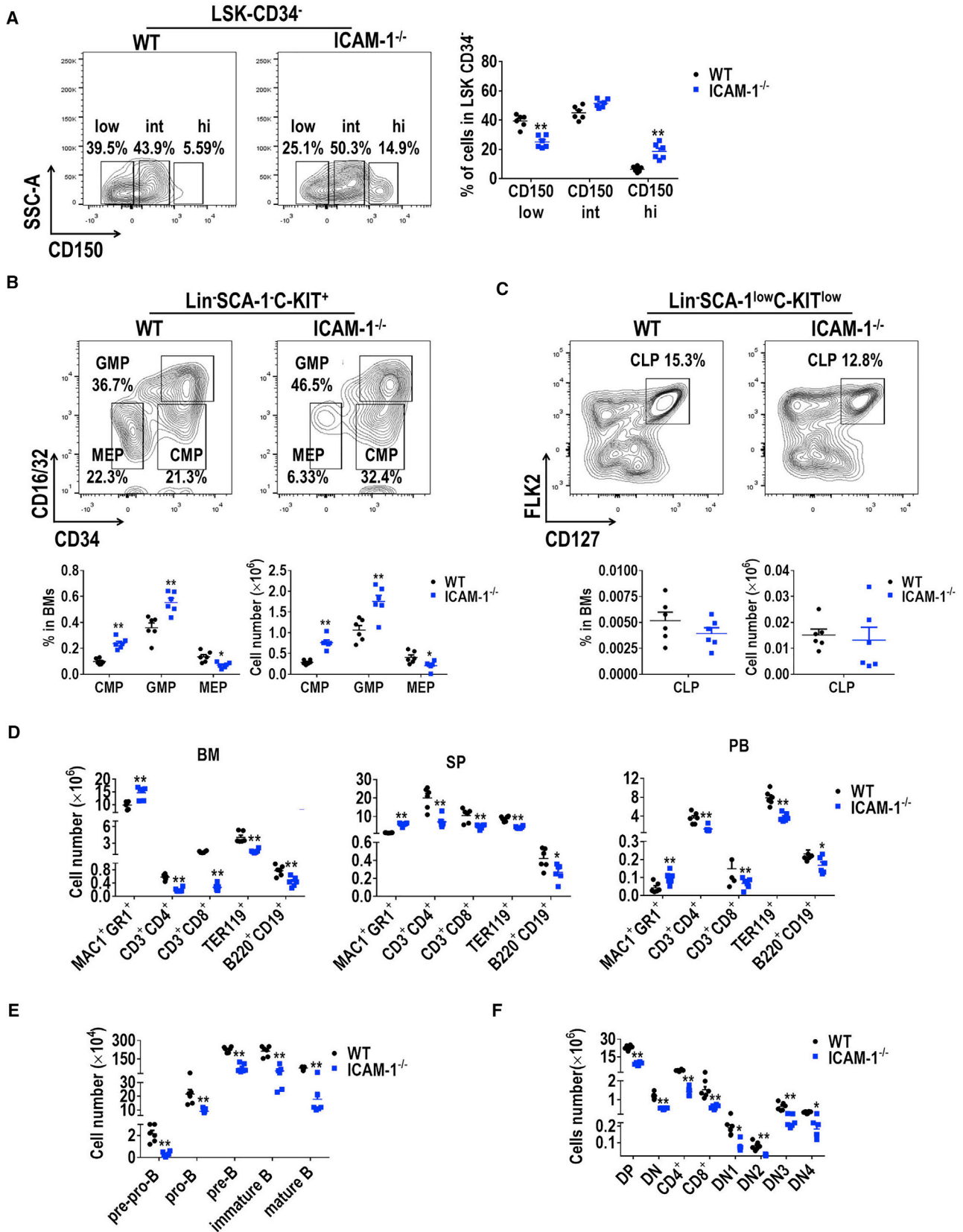
(legend on next page)

higher proliferative status, *cyclinD1* (*Ccnd1*) expression was upregulated, whereas multiple negative regulators of cell proliferation, including cyclin-dependent kinase inhibitors p21 (*Cdkn1a*), p27 (*Cdkn1b*), and *Nurr1* (*Nr4a2*), were downregulated in ICAM-1$^{-/-}$ HSC^{-LT} (Figure 1D). In contrast, no difference in cycling rate was observed for HSC^{-ST} and MPPs derived from WT and ICAM-1$^{-/-}$ mice (Figures S1E and S1F). The apoptotic rate of distinct populations of HSPCs did not differ between WT and ICAM-1$^{-/-}$ mice (Figure S1G), suggesting that ICAM-1 did not affect the survival of HSPCs. These results collectively demonstrate that loss of ICAM-1 causes expansion of phenotypic HSC^{-LT} with impaired quiescence under steady-state conditions.

Cycling HSCs are more vulnerable to 5-fluorouracil (5-FU) cytotoxicity, whereas quiescent HSCs remain viable after 5-FU treatment (Cheng et al., 2000). ICAM-1$^{-/-}$ mice challenged with sequential 5-FU dose died dramatically faster than WT controls: 70% of ICAM-1$^{-/-}$ mice succumbed at 14 days and all remaining mice died at 20 days after initiation of 5-FU injection. In contrast, only 20% of WT mice succumbed at 14 days and 50% died at 23 days after 5-FU injection (Figure 1E). Analysis of another cohort of 5-FU-treated mice showed that HSC^{-LT} from ICAM-1$^{-/-}$ mice were less efficient at replenishing bone marrow cells and hematopoietic progenitor cells (HPCs) and tended to become exhausted (Figure 1F). These observations support the importance of ICAM-1 in the maintenance of HSC^{-LT} quiescence.

ICAM-1 Deficiency Favors Myeloid Cell Expansion

Next, we studied whether the absence of ICAM1 affects the differentiation potential of HSCs. Distinct populations within the HSC pool present different lineage differentiation potentials, which could be distinguished by diverse levels of CD150 (SLAM) expression: CD150^{hi}, CD150^{int}, and CD150^{low} (Beerman et al., 2010; Kent et al., 2009; Morita et al., 2010). Flow cytometric analysis revealed a substantial change in the levels of HSC compartments upon ICAM-1 deletion: the proportion of CD150^{hi} in the ICAM-1$^{-/-}$ HSC (LSK-CD34$^-$) pool was more than 2-fold higher than in WT littermates (7.75% ± 1.79% in WT

versus 20.6% ± 5.20% in ICAM-1$^{-/-}$), whereas the CD150^{low} subset decreased to half that of WT controls (42.5% ± 8.76% in WT versus 22.3% ± 4.20% in ICAM-1$^{-/-}$) (Figure 2A). We further evaluated the levels of lineage-committed progenitors. Flow cytometric analysis showed that the proportion and absolute cell counts of common myeloid progenitors (CMPs) and granulocyte/monocyte progenitors (GMPs) were significantly elevated, whereas megakaryocyte-erythroid progenitors (MEPs) were dramatically decreased in ICAM-1$^{-/-}$ mice compared with WT controls (Figure 2B). However, the frequencies of common lymphoid progenitors (CLPs) displayed no variation (Figure 2C). These changes in lineage specification were accompanied by an expansion of immature myeloid cells (MAC1$^+$GR1$^+$), as well as lower levels of lymphocytes (T and B cells) and erythrocytes (Ter119$^+$) in the bone marrow, spleen, and peripheral blood of ICAM-1$^{-/-}$ mice compared with their WT littermates (Figure 2D). In addition to the lower levels of lymphocytes, further analysis showed a systematic reduction of developing B cells in the bone marrow (Figure 2E) and the reduction of different stages of T lymphocytes in the thymus of ICAM-1$^{-/-}$ mice (Figure 2F). Complete blood count analysis of key hematological parameters revealed higher neutrophil levels but fewer lymphocytes, and a substantial drop in the levels of red blood cells, hemoglobin, and platelets in ICAM-1$^{-/-}$ mice (Table S1). These observations indicate that loss of ICAM-1 favors myeloid cell expansion.

HSCs with ICAM-1 Deletion Display Normal Quiescence and Transplantation Capability after Transplantation

Based on the observation that ICAM-1 could regulate the quiescence of HSCs, we sought to determine whether this was intrinsic to HSCs or was mediated by the bone marrow niche. It should be noted that ICAM-1 is expressed on both hematopoietic cells and major bone marrow niche cells, including endothelial cells (Ecs), mesenchymal stem cells (Msc), osteoblasts (Obs), and CXCL12-abundant reticular cells (CARs) (Figure S2A). First, serial competitive transplantation experiments were performed: HSC^{-LT} from WT or ICAM-1$^{-/-}$ mice (donor, Ly5.2$^+$) were mixed with

Figure 2. ICAM-1 Deficiency Favors Myeloid Cell Expansion

(A) Flow cytometric analysis of HSC compartments based on CD150 expression in bone marrow from WT and ICAM-1$^{-/-}$ mice. Both representative profile (left) and data are shown as the mean ± SEMs from three independent experiments (n = 6, right).

(B and C) Flow cytometric analysis of CMPs, GMPs, MEPs (B) and CLPs (C) in bone marrow from WT and ICAM-1$^{-/-}$ mice. Both representative profile (upper) and data are shown as the mean ± SEMs from three independent experiments (n = 6, lower).

(D) Absolute number of distinct mature cells in bone marrow (BM), spleen (SP), and peripheral blood (PB), including myeloid cells (MAC1$^+$GR1$^+$), T cells (CD3$^+$CD4$^+$/CD3$^+$CD8$^+$), B cells (B220$^+$CD19$^+$), and erythrocytes (TER119$^+$), in WT and ICAM-1$^{-/-}$ mice.

(E and F) Absolute number of developing B cells in bone marrow (E) and developing T cells in thymus (F) from WT and ICAM-1$^{-/-}$ mice. Data are shown as the mean ± SEMs from three independent experiments (n = 6).
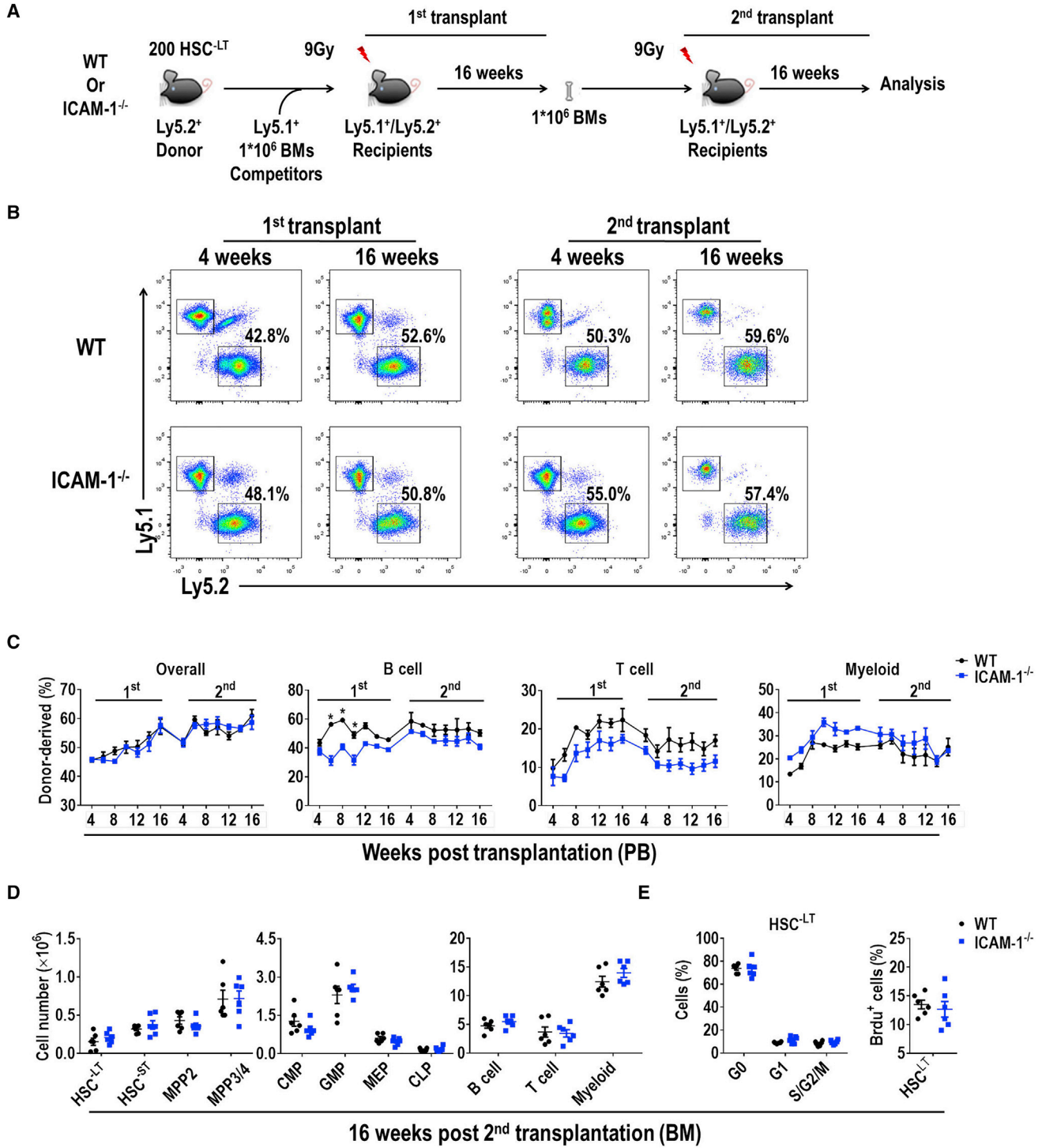
*p < 0.05; **p < 0.01.

Figure 3. HSCs with ICAM-1 Deletion Display Normal Quiescence and Transplantation Capability after Transplantation

(A) Experimental schematic for serial competitive transplantation with HSC^{-LT} from WT and ICAM-1$^{-/-}$ mice (n = 6); results in (B)–(E).

(B) Representative flow cytometric profiles of chimerism in peripheral blood at the indicate time points.

(C) Dynamic analysis of donor-derived cells in peripheral blood (PB) at the indicated time points.

(legend continued on next page)

bone marrow cells from congenic mice (competitor, Ly5.1$^+$), followed by transplantation into lethally irradiated recipients (Ly5.1$^+$/Ly5.2$^+$). The secondary transplantation was performed 16 weeks later; bone marrow cells were harvested from the primary recipient mice and were transplanted into a secondary set of lethally irradiated animals (Figure 3A). Deletion of ICAM-1 in HSC^{-LT} did not affect their repopulation capabilities (Figure 3B). As expected, WT HSC^{-LT} gave rise to stable long-term multi-lineage reconstitution in peripheral blood in recipient mice. No difference was observed between ICAM-1$^{-/-}$ and WT control up until 16 weeks after secondary transplantation, except a transitory defect in B cell engraftment during the first transplantation with ICAM-1$^{-/-}$ HSC^{-LT} (Figure 3C). Flow cytometric analysis revealed no difference in the frequencies of distinct HSPCs, lineage-committed progenitors, and mature cells in the bone marrow (Figure 3D). No change was observed in the proliferative status of HSC^{-LT} derived from ICAM-1$^{-/-}$ and WT mice (Figure 3E). Conditional deletion of ICAM-1 (*ICAM-1$^{f/f}$;Vav1-Cre*) in hematopoietic cells by breeding *ICAM-1$^{f/f}$* mice with *Vav1-Cre* transgenic mice failed to cause any noticeable effects on the HSC compartment (Figures S3A–S3F).

ICAM-1 Deficiency in the Niche Regenerates HSCs with Defective Quiescence and Transplantation

Next, we performed reciprocal transplantation to investigate whether these defects were mediated by the bone marrow niche. As shown in Figure S4A; Ly5.2$^+$ WT bone marrow was transplanted into lethally irradiated Ly5.1$^+$ WT mice (WT-to-WT, blue), Ly5.2$^+$ ICAM-1$^{-/-}$ bone marrow was transplanted into lethally irradiated Ly5.1$^+$ WT mice (ICAM-1$^{-/-}$-to-WT, red), Ly5.1$^+$ WT bone marrow was transplanted into lethally irradiated Ly5.2$^+$ ICAM-1$^{-/-}$ mice (WT-to-ICAM-1$^{-/-}$, green), and Ly5.2$^+$ ICAM-1$^{-/-}$ bone marrow was transplanted into lethally irradiated Ly5.2$^+$ ICAM-1$^{-/-}$ mice (ICAM-1$^{-/-}$-to-ICAM-1$^{-/-}$, purple). At 8 weeks post transplantation, bone marrow analysis revealed a systematic decline in absolute cell counts of HSPCs population, lineage-determined progenitors, as well as mature cells in ICAM-1$^{-/-}$ recipients compared with WT controls (Figure S4B). These changes were accompanied by a higher level of proliferative HSC^{-LT} (Figure S4C). However, the defects of WT bone marrow transplants into ICAM-1$^{-/-}$ recipients (green) failed to persist for a long time; indeed, the parameters were restored to levels comparable with those of WT recipients at 16 weeks

post transplantation (Figures S4D and S4E). When ICAM-1$^{-/-}$ bone marrow was transplanted into ICAM-1$^{-/-}$ recipients (purple), defects in reconstitution and proliferative of HSC^{-LT} were persistently observed (Figures S4D and S4E). These observations indicate that the transplanted WT bone marrow niche could gradually reconstitute the bone marrow microenvironment in ICAM-1$^{-/-}$ mice (Liang et al., 2013). To further confirm this possibility, WT hematopoietic cells (HEM: CD45$^+$/TER119$^+$) were combined with non-hematopoietic cells (non-HEM: CD45$^-$/TER119$^-$) from WT (black) or ICAM-1$^{-/-}$ (red) mice, followed by transplantation into lethally irradiated ICAM-1$^{-/-}$ recipients (Figure 4A) (Liang et al., 2013). Genotyping proved the presence of donor-derived non-hematopoietic cells in the recipients (Figure S4F). Significant defects in long-term reconstitution, as well as a dramatic expansion of myeloid cells and a lower proportion of lymphocytes, were observed in donor hematopoietic cells combined with ICAM-1$^{-/-}$ non-HEM in the serial transplantation (Figures 4B and 4C). Recipients transplanted with donor hematopoietic cells combined with ICAM-1$^{-/-}$ non-HEM also displayed a remarkable reduction in HSPCs, lineage-defined progenitors, and mature cells in the bone marrow (Figure 4D), as well as an expected higher proportion of cycling HSC^{-LT} (Figure 4E). Consistently, when ICAM-1$^{-/-}$ HSC^{-LT} was combined with non-HEM (CD45$^-$/TER119$^-$) from WT (black) or ICAM-1$^{-/-}$ (red) mice, similar results were observed (Figures S5A–S5C). Further hematopoietic colony-forming units (CFUs) assay showed that WT HSPCs (Lin$^-$) gave smaller colony numbers after co-culture with stromal cells with ICAM-1 deletion (Figure S5D). Collectively, these observations support the notion that ICAM-1 deficiency in niche regenerates HSCs with defective quiescence and repopulation, as noted in ICAM-1$^{-/-}$ mice.

The Mechanism Responsible for Defective HSCs Is Traced to the ICAM-1$^{-/-}$-Derived Niche

Retention of HSCs in the bone marrow is a prerequisite for maintaining their biological function (Mendelson and Frenette, 2014). This is reflected by the capability of HSCs to be mobilized from the bone marrow in response to stimulation, as well as efficient homing to bone marrow upon transplantation (Xing et al., 2006). Based on our observations that ICAM-1 regulated HSC function in a niche-dependent manner, we speculated that ICAM-1 might affect the retention of HSCs in the bone marrow. We

(D) Absolute number of donor-derived HSPCs, progenitors, and mature cells in bone marrow (BM) at 16 weeks after second transplantation.
(E) Cell-cycle (left) and BrdU analysis (right) of donor-derived HSC^{-LT} in bone marrow at 16 weeks after second transplantation. Mean ± SEMs were shown.
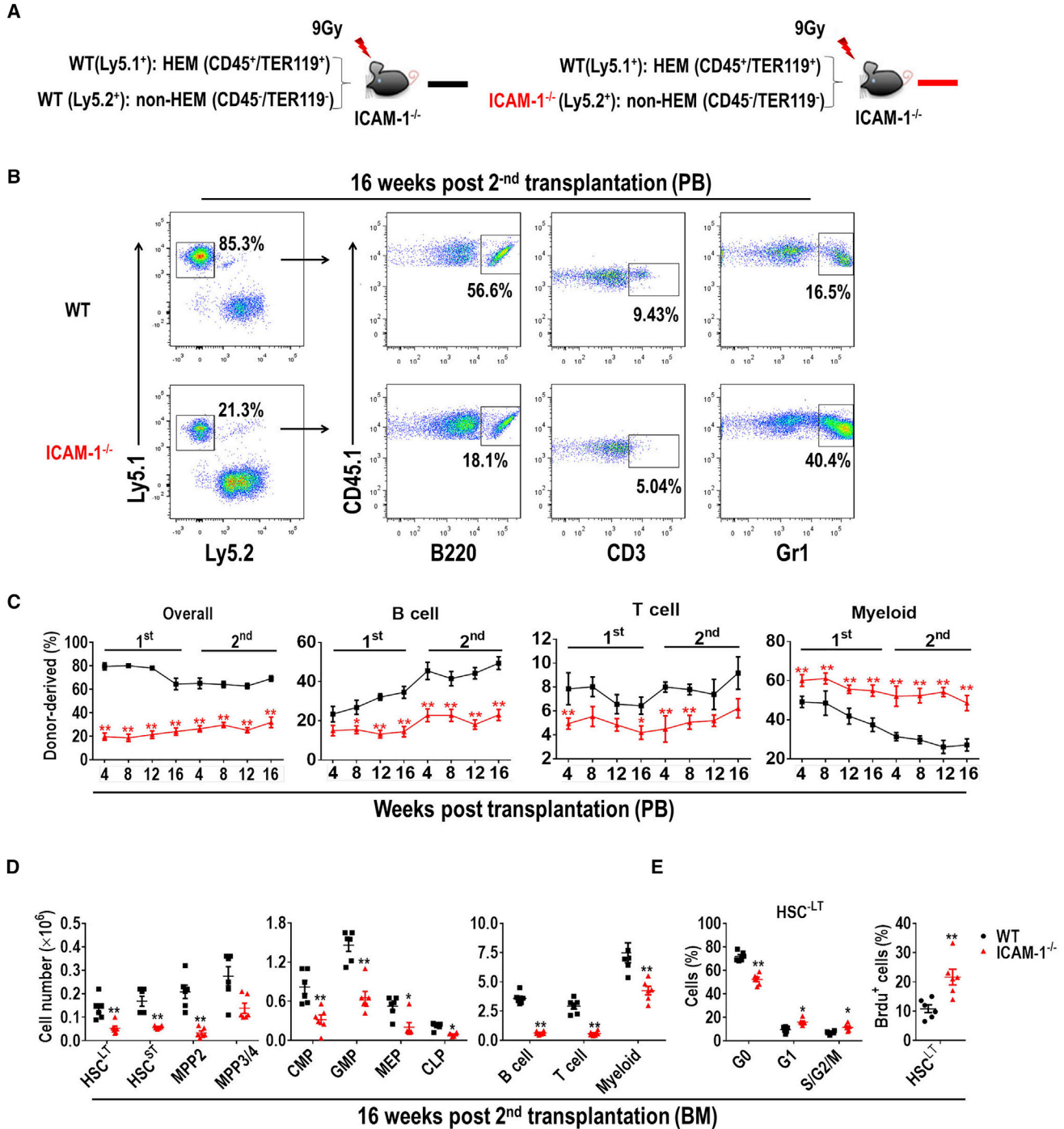*p < 0.05.

Figure 4. ICAM-1 Deficiency in Niche Regenerates HSCs with Defective Quiescence and Transplantation

(A) Experimental schematic for the mixture transplantation: WT hematopoietic cells (WT: HEM) were combined with non-hematopoietic cells (non-HEM) from WT (black) or ICAM-1$^{-/-}$ (red), followed by transplantation into ICAM-1$^{-/-}$ mice (n = 6); results in (B)–(E).

(B) Representative flow cytometric profiles of chimerism and proportions of donor-derived cells in peripheral blood at 16 weeks after second transplantation.

(C) Dynamic analysis of donor-derived cells in peripheral blood (PB) at the indicated time points.

(legend continued on next page)

performed a standard mobilization experiment by intraperitoneal injection of granulocyte colony-stimulating factor (G-CSF), the regimen used for clinical HSC mobilization (Chitteti et al., 2014). Spleen cellularity (Figure 5A) and absolute cell number of LSK in the spleen (Figure 5B) were significantly higher in ICAM-1$^{-/-}$ than WT animals upon G-CSF administration. Elevation of circulating clonogenic progenitors in ICAM-1$^{-/-}$ mice was confirmed by a CFU assay (Figure 5C). Similar results were observed in peripheral blood (Figures S6A and S6B). These findings indicated that ICAM-1 deletion may facilitate HSC mobilization to peripheral tissues. We next determined whether ICAM-1 deletion in the niche could impair the adhesive properties of HSPCs. HSPCs from WT mice were plated on top of distinct stroma cells derived from WT or ICAM-1$^{-/-}$ mice, including Msc, CAR, Ecs, and Obs. Results showed that WT HSPCs showed a clear reduction in their adhesive ability upon co-culture with ICAM-1$^{-/-}$-derived Ecs or Obs, but no effects were observed for Msc or CAR (Figure 5D). Similar defects were observed when ICAM-1$^{-/-}$-derived HSPCs were made to adhere to stroma cells from ICAM-1$^{-/-}$ mice (Figure S6C). Accordingly, ICAM-1 expression in Ecs and Obs niche cells could promote HSC adhesion. Meanwhile, the homing index of HSC^{-LT} to ICAM-1$^{-/-}$ recipients was lower than in the case of WT recipients, whereas no defects were observed for other subsets of HSPCs (Figure 5E). In addition, HSCs from ICAM-1$^{-/-}$ mice resided closer to the central vein, compared with WT littermates (Figure S6D), which might indicate easier mobilization to the peripherals. These results suggest that ICAM-1 expression in certain types of stroma cells plays an important role in facilitating retention of HSCs in the bone marrow.

Although flow cytometric analysis failed to reveal any difference in the levels of distinct stroma cells between WT and ICAM-1$^{-/-}$ mice, including Ecs, Msc, Obs, and CAR (Figure 5F), HSC^{-LT} displayed higher proliferation upon co-culture with Obs and Ecs from ICAM-1$^{-/-}$ mice, including both Ki67 staining (Figure 5G) and BrdU staining (Figure S6E). No noticeable differences were observed upon co-culture with Msc or CAR (Figures 5G and S6E). Further gene expression analysis showed that cytokines important for HSC maintenance, such as stem cell factor (*Scf*), stromal cell-derived factor-1 (*Sdf-1*), and angiopoietin 1(*Ang-1*) in Obs, or *Scf* and *Ang-1* in Ecs, were significantly downregulated upon ICAM-1 deficiency (Figures 5H and 5I). Instead, cytokines responsible for promoting HSC mobilization and myeloid cell differentiation, including *G-csf*, granulocyte-macrophage colony-stimulating factor (*Gm-csf*), and chemokine (C-C motif) ligand 5 (*Ccl5*), were significantly upregulated in ICAM-1$^{-/-}$-derived Obs, and the expression of *G-CSF*, transforming growth factor β (*Tgf-β*), and *Ccl5* were also upregulated in ICAM-1-deficient Ecs (Figures 5H and 5I). These observations indicate that loss of ICAM-1 in niche affected the production of stromal cell-derived cytokines and chemokines, which may contribute to their defects. To gain insight into the mechanism, WT donor LSK (Ly5.1$^+$) were sorted after transplanted into WT or ICAM-1$^{-/-}$ recipients (Ly5.2$^+$) for 8 weeks. High-throughput RNA sequencing was performed to evaluate the transcriptional profile. A total of 564 genes with more than 2-fold difference were identified (Figure S7A). Among the differentially expressed genes, those related to HSC stemness, cell adhesion, and cell cycle were most changed (Figure S7B), and were validated by qRT-PCR (Figures S7C–S7E). These results indicated that ICAM-1 deficiency in the bone marrow niche may elicit intracellular reprogramming of HSCs.

Significance of ICAM-1 Expression in the Human Bone Marrow Niche

To determine the potential significance of ICAM-1 in human HSCs, we first evaluated ICAM-1 expression in niche stroma cells (CD45$^-$/Lin$^-$) from human bone marrow. Flow cytometric analysis showed that stroma cells expressed relatively high levels of ICAM-1 (Figure 6A). Neutralization of ICAM-1 significantly increased the level and proliferation of primitive HSCs when co-cultured with bone marrow stroma cells (Figure 6B). Expression of several cyclin-dependent kinase inhibitors, including P16 (*CDKN2A*), P21 (*CDKN1A*), and P27 (*CDKN1B*), was consistently downregulated upon anti-ICAM-1 treatment (Figure 6C). These observations supported the functional requirement of ICAM-1 for human HSCs. Loss of quiescence in HSCs and their detachment from the niche lead to expansion of myeloid progenitors in human chronic myeloid leukemia (CML) (Bruns et al., 2009). Bone marrow stroma cells from myelocytic leukemia (CML [chronic myeloid leukemia] and AML [acute myeloid leukemia]) patients expressed ICAM-1 at a much lower level than healthy donors, both at mRNA and protein levels (Figures 6D and 6E). Although no differences were observed for lymphocytic leukemia (ALL [acute lymphoblastic leukemia] and CLL [chronic lymphoblastic leukemia]) (Figures 6D

(D) Absolute number of donor-derived HSPCs, progenitors, and mature cells in bone marrow (BM) at 16 weeks after second transplantation.
(E) Cell-cycle (left) and BrdU analysis (right) of donor-derived HSC^{-LT} in bone marrow at 16 weeks after second transplantation. Mean ± SEMs were shown.
*p < 0.05; **p < 0.01.
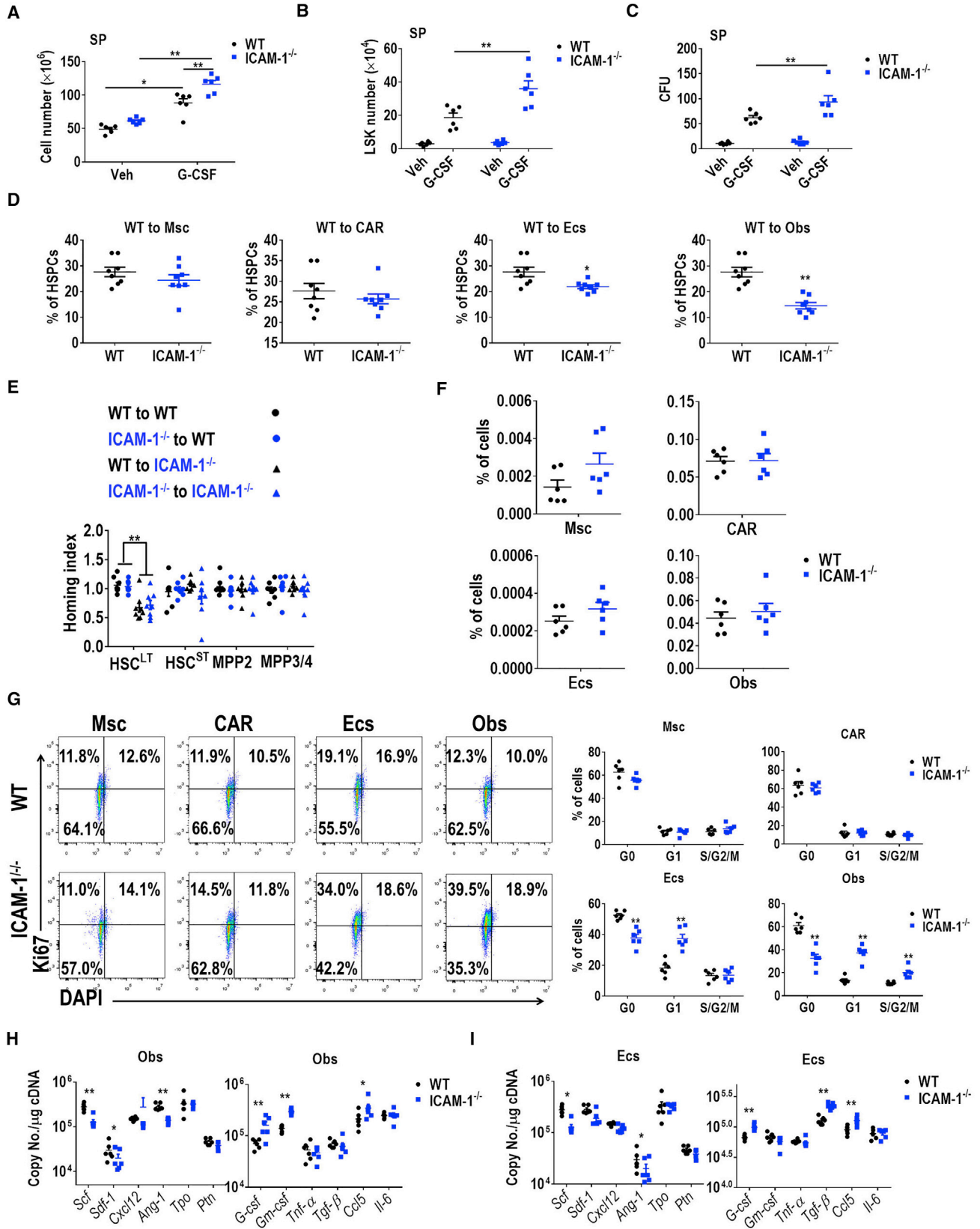
(legend on next page)

and 6E). Furthermore, co-culture with stromal cells with ICAM-1 overexpression suppressed the proliferation of CML-derived HSCs, compared with normal stromal cells (Figures 6F and 6G). These observations indicate that ICAM-1 expression in stroma cells might regulate HSC function and participates in the progression of myelocytic leukemia.

DISCUSSION

In this study, we have identified ICAM-1 as a contributory regulator of HSCs, whose action is bone marrow niche dependent. Deficiency of ICAM-1 in the bone marrow niche causes expansion of long-term HSCs characterized by impaired quiescence and repopulation capability, as well as myeloid cell expansion. Changes in HSC retention in the bone marrow and stroma-derived factor expression profiles represent the potential mechanisms underlying this phenomenon.

Bone marrow transplantation showed that HSCs from ICAM-1$^{-/-}$ mice displayed similar engraftment potential to WT controls, upon transplantation into WT hosts, whereas ablation of ICAM-1 in the bone marrow niche impaired the long-term repopulation and quiescence of long-term HSCs, as shown by the reciprocal bone marrow transplantation and transplantation of combined hematopoietic cells with non-hematopoietic cells. The defects in HSC repopulation caused by the ICAM-1-deficient niche even persisted until 16 weeks after the second transplantation. However, it is possible that the donor-derived stromal cells may exert their effect early in the transplantation period and have long-lasting functional consequences on the transplanted HSCs and their progeny. These results support that the observed defects of HSCs from ICAM-1$^{-/-}$ mice were non-cell-autonomous defects, rather than intrinsic to HSCs. Moreover, these defects were reversible, depending on the presence or absence of ICAM-1 in niche cells.

ICAM-1 deficiency in the niche did not affect the levels of distinct stroma cells. Factors production from Obs and Ecs were altered, which may contribute to defective HSC function. Elevated expression of G-CSF and Ccl5 in the ICAM-1-null niche may facilitate HSC mobilization and myeloid cell differentiation (Akashi et al., 2000; Ergen et al., 2012; Schepers et al., 2012; Suh et al., 2009), whereas downregulation of Scf and Ang1 may be related to impaired HSC maintenance (Itkin and Lapidot, 2011; Zhang et al., 2006). We observed that ICAM-1 deficiency in mice led to increased HSC mobilization, which supports the essential role of the bone marrow niche in ICAM-1-mediated HSC mobilization. Understanding the exact mechanism underlying ICAM-1 function in HSCs, however, will require deletion of ICAM-1 in specific stromal cell lineages.

The HSC pool is composed of different populations that display distinct lineage potentials and could be distinguished by CD150 expression (Dykstra et al., 2011; Beerman et al., 2010). Flow cytometric analysis revealed that ICAM-1$^{-/-}$ mice displayed a markedly higher ratio of myeloid cells versus lymphoid cells. The proportions of progenitors, such as GMPs, CMPs, and MEPs, were consistently altered. These led to significantly higher levels of myeloid cells and compensatory fewer T and B lymphocytes in ICAM-1$^{-/-}$ mice. Besides their decreased self-renewal potential, one of the hallmarks of aging HSCs is skewing toward myeloid cells (Geiger et al., 2014; Chambers et al., 2007). The expansion of myeloid cells, as well as impaired HSC quiescence in ICAM-1-deficient mice, raises the possibility that deficient ICAM-1 expression in the niche may be

Figure 5. The Mechanism Responsible for Defective HSCs Is Traced to the ICAM-1$^{-/-}$-Derived Niche
(A–C) Mobilization assay: G-CSF was administered intraperitoneally to WT and ICAM-1$^{-/-}$ mice (12.5 g/kg body weight, daily) for 5 days (n = 6). Total splenocytes (A), numbers of LSKs (B), and CFU counts (C) in 10^5 splenocytes (SP) were measured.
(D) Adhesion assay: HSPCs from WT mice were plated on the top of stroma cells from WT or ICAM-1$^{-/-}$ mice, including Msc, CAR, Ecs, and Obs, and non-adhesive cells were washed off after 2 hr (n = 8). The percentages of HSPCs adherent to stroma cells were evaluated by flow cytometry.
(E) Homing assay: bone marrow cells (2 × 10^7) from either WT or ICAM-1$^{-/-}$ mice were labeled with CFSE and used as donor cells for homing assay. The proportions of HSPCs before (R1) and after (R2) transplantation were analyzed by flow cytometry. The homing index was calculated based on the ratio of R2 to R1. Mean ± SEMs from six mice in each groups were shown.
(F) Frequency of stroma cells in bone marrow from WT and ICAM-1$^{-/-}$ mice, including Msc, Ecs, Obs, and CAR.
(G) Purified WT HSPCs were co-cultured with distinct stroma cells from WT and ICAM-1$^{-/-}$ mice for 10–12 days, and the cycling status of HSC^{-LT} was evaluated by flow cytometry. Both representative results (left) and mean ± SEMs from three independent experiments (right) were shown.
(H and I) Expression of indicated genes, including stem cell factor (Scf), stromal cell-derived factor-1 (Sdf-1), chemokine (C-X-C motif) ligand 12 (Cxcl12), angiopoietin 1(Ang-1), thrombopoietin (Tpo), pleiotrophin (Ptn), granulocyte colony-stimulating factor (G-csf), granulocyte-macrophage colony-stimulating factor (Gm-csf), tumor necrosis factor alpha (Tnf-α), transforming growth factor β (Tgf-β), chemokine (C-C motif) ligand 5 (Ccl5), and interleukin 6 (Il6) were analyzed by absolute quantification real-time PCR in purified Obs (H) and Ecs (I). Mean ± SEMs from three independent experiments were included.
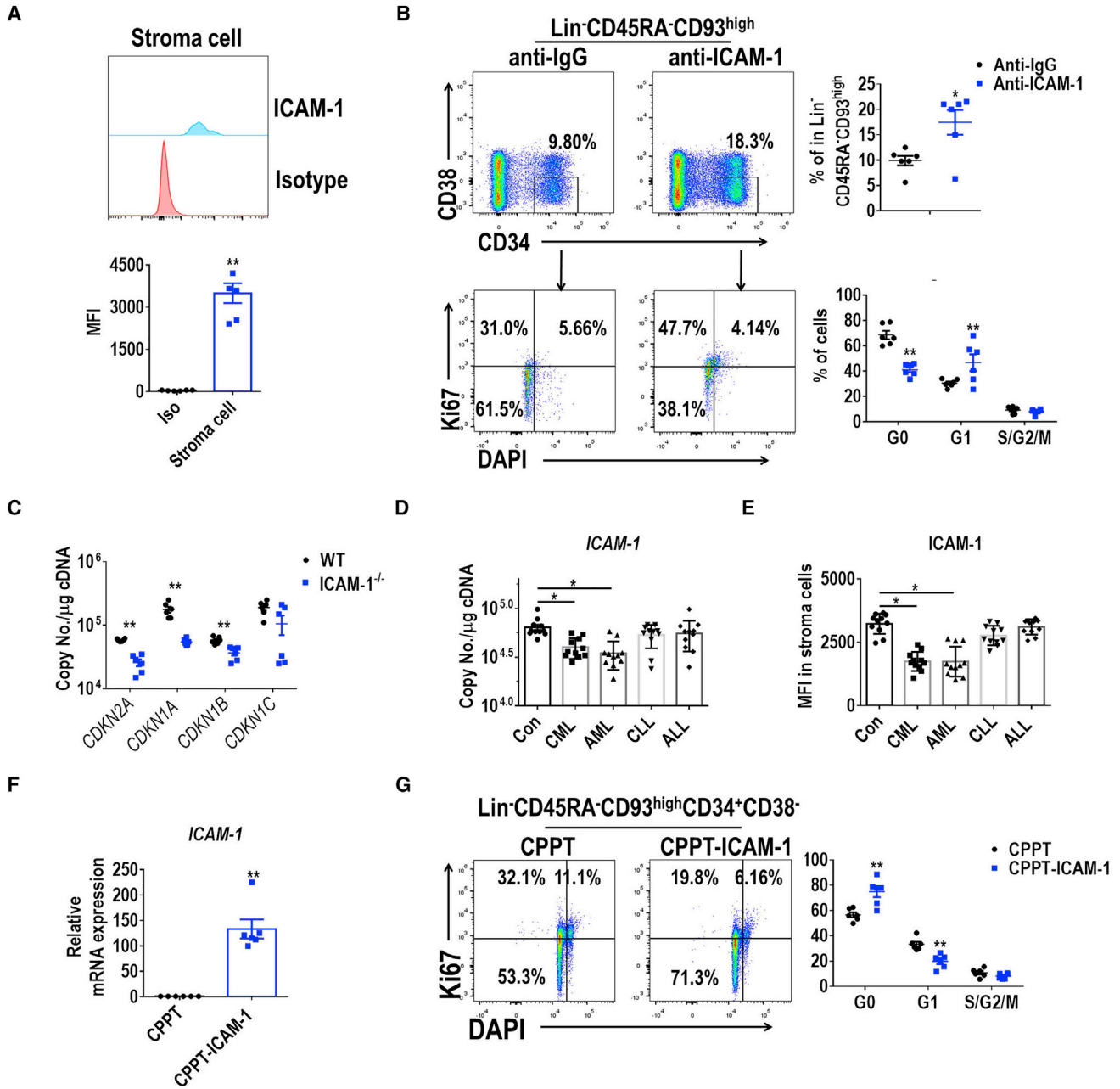*p < 0.05; **p < 0.01.

Figure 6. Significance of ICAM-1 Expression in Human Bone Marrow Niche

(A) Flow cytometric analysis of ICAM-1 expression in stroma cells (CD45$^-$/Lin$^-$) from bone marrow of healthy donors (n = 6). Both representative results (upper) and mean ± SEMs of mean fluorescence index (MFI) (lower) were shown.

(B) Human HSPCs (Lin$^-$ cells) were co-cultured with bone marrow stroma cells in the presence of anti-ICAM-1 or anti-IgG. Flow cytometric analysis of primitive HSCs (Lin$^-$CD45RA$^-$CD93^{high}CD38$^-$CD34$^+$) (upper) and their cell-cycle status (lower) are shown. Both representative results (left) and mean ± SEMs (right) from six independent experiments were included.

(C) The expression levels of cell-cycle-related genes from samples in (B) were evaluated by absolute quantification real-time PCR.

(D and E) ICAM-1 expression in bone marrow stroma cells from healthy donors and CML, AML, ALL, and CLL patients (n = 11) was analyzed by absolute quantification real-time PCR (D) and flow cytometry (E).

(F) Bone marrow stroma cells were infected with lentivirus with control vector (central polypurine tract [CPPT]) or ICAM-1 overexpression (CPPT- ICAM-1). ICAM-1 expression was measured by infected absolute quantification real-time PCR.

(legend continued on next page)

associated with HSC aging. Our preliminary results showed that young ICAM-1$^{-/-}$ mice displayed similar changes in HSPCs to aged WT mice, including higher levels of phenotypic HSC^{-LT}, CD150^{hi}-HSCs, and myeloid cells (our unpublished data), indicating that HSCs from ICAM-1$^{-/-}$ mice displayed a phenotype of aging. The reduced homing capability and enhanced mobilization further support this possibility. Further investigation is needed to study the detailed role of ICAM-1 in HSC aging.

The capability of HSC retention in the bone marrow is a prerequisite for proper HSC function (Nilsson et al., 2001). Immunofluorescence staining showed that HSCs from ICAM-1$^{-/-}$ mice resided closer to the central vein compared with WT littermates. It was reported that quiescent HSCs are adjacent to the endosteal niche, whereas activate HSCs are surround by sinusoids (Mendelson and Frenette, 2014). Our result indicates that alteration of HSC location within the bone marrow microenvironment may be relevant to their impaired functionality in ICAM-1$^{-/-}$ mice. Furthermore, the interplay between HSCs and stroma cells, mediated through adhesion receptors and their ligands, is also critically important for HSC retention in the bone marrow. ICAM-1 is expressed at higher levels in specific stroma cells (such as Ecs), whereas its ligand LFA-1 was dominantly expressed in hematopoietic cells (HSPCs) in the bone marrow niche (Figure S2B). It is plausible that binding of ICAM-1 expressed on stroma cells with LFA-1 on HSCs facilitates the proper retention of HSCs in the bone marrow, thus contributing to their maintenance. It was reported that anti-LFA-1 treatment could significantly reduce the levels of engraftment of human CD34$^+$ cells (Peled et al., 2000). It is therefore possible that interaction between HSCs and niche cells mediated by ICAM-1 and LFA-1 could regulate HSC functionality. This interaction may modulate the capability of HSC retention in the bone marrow or lead to alterations in stroma-derived cytokine production, which eventually contribute to HSC maintenance. Interestingly, even the expression of LFA-1 in HSC^{-LT} was comparable with other types of HSPCs; HSC^{-LT} under quiescence (G0 phase) expressed a significantly higher level of LFA-1 compared with cycling HSCs (Figures S2C–S2D). These results support the importance of LFA-1 in the maintenance of HSC^{-LT} quiescence. The detailed mechanism of ICAM-1/LFA-1 axis-mediated regulation of HSC, however, remains to be fully understood.

RNA sequencing analysis revealed that LSK, upon interaction with ICAM-1-deficient niche, showed dramatic changes in the profile of transcription: genes related to cell adhesion (such as *Rtn4*, *Wafs2*, *Mef2c*, and *Arhgef1*) and HSC stemness (*Satb1*, *Runx1*, *Notch1*) were significantly downregulated, while several positive cell-cycle regulators (*Cdk1*, *Cdc45*) were upregulated. These results indicate that ablation of ICAM-1 in stroma cells leads to reprogramming of the intracellular signaling events in HSCs.

The significant changes in hematological parameters caused by niche ICAM-1 deficiency may have clinical relevance in hematopoietic disease, such as myelocytic leukemia. It was reported that mice with deletion of ICAM-1 and P selectin developed BCR/ABL-induced CML-like leukemia at a significantly faster rate than control littermates (Pelletier et al., 2004). We found that the expression of ICAM-1 in bone marrow stroma of myelocytic leukemia patients was significantly lower than that in healthy donors, indicating a potential pathological significance of ICAM-1 in myelocytic leukemia diseases.

In summary, our study identifies a regulatory mechanism whereby niche ICAM-1 preserves HSC functions. These findings will improve our understanding of how the niche contributes to HSC maintenance, which may lead to a therapeutic strategy to enhance bone marrow transplantation and treatment of leukemia in the future.

EXPERIMENTAL PROCEDURES

Mice

ICAM-1$^{-/-}$ mice (B6.129S4-Icam1tm1Jcgr/J) were purchased from Jackson Laboratory. Age- and gender-matched WT littermates were used as controls. *ICAM-1$^{f/f}$* mice were generated in Nanjing Biomedical Research Institute of Nanjing University (China), and crossed to *Vav1-Cre* transgenic mice (Jackson Laboratory) to produce the conditional knockout mouse (*ICAM-1$^{f/f}$;Vav1-Cre*). The recipient mice used in bone marrow transplantation assays were Ly5.1$^+$/Ly5.2$^+$ (CD45.1$^+$CD45.2$^+$) heterozygotes. All animal experiments in this study were approved by The Animal Care and Ethics Committee of Sun Yat-sen University. All animals were maintained under specific pathogen-free conditions and fed with standard diet.

Flow Cytometric Analysis and Cell Sorting

Single-cell suspensions were prepared, and red blood cells were lysed. For staining, cells were washed once with fluorescence-activated cell sorting (FACS) buffer (0.1% BSA in PBS), and then 10^6 cells were resuspended in 200 μL of FACS buffer for the following staining using 1:200 dilutions of primary antibodies unless otherwise indicated. Flow cytometric analysis was performed with a BD

(G) Bone marrow stroma cells with ICAM-1 overexpression were co-cultured with CML patient-derived HSPCs (Lin$^-$ cells) for 10 days, and cell cycle of primitive HSCs was determined by flow cytometric analysis. Both representative results (left) and data are shown as the mean ± SEMs from three independent experiments (n = 6).
*p < 0.05; **p < 0.01.

LSRFortessa cell analyzer (BD Biosciences, San Jose, CA), and data were analyzed with FlowJo software (Tree Star, Ashland, OR). All antibodies are identified in the Supplemental Information (Tables S2 and S3).

Bone Marrow Transplantation Experiment

For serial competitive transplantation, 200 HSC^{-LT} from WT and $ICAM-1^{-/-}$ donor mice ($Ly5.2^+$) were mixed with 1×10^6 bone marrow cells from age-matched WT mice (competitor, $Ly5.1^+$), and injected into lethally irradiated recipient mice ($Ly5.1^+$/$Ly5.2^+$). For secondary transplantation, 1×10^6 chimeric bone marrow cells from the primary recipients were transplanted into the secondary recipient ($Ly5.1^+$/$Ly5.2^+$) mice 16 weeks after primary transplantation.

5-FU Treatment

WT and $ICAM-1^{-/-}$ mice (10–12 weeks) were intraperitoneally injected with a single dose (150 mg/kg body weight) of 5-FU. Mice were then euthanized at different time points, and bone marrow cells were isolated and counted. The proportions of HSPCs ($Lin^-SCA-1^-C-kIT^+$) were analyzed by flow cytometry and then multiplies by the absolute number of bone marrow cells to calculate the absolute number of HSPCs. For serial 5-FU treatments, mice were injected intraperitoneally with 5-FU (150 mg/kg body weight) weekly, and survival was monitored daily.

Cell-Cycle Analysis

Bone marrow cells were first stained with specific cell surface markers for HSPC subpopulations, then fixed and permeabilized using the Cytofix/Cytoperm Fixation/Permeabilization Kit (BD) according to manufacturer's instructions. Cells were then stained with Ki67 fluorescein isothiocyanate (1:100 in BD Perm/Wash buffer for 30 min)/DAPI (2 μg/mL for 10 min prior to analysis) or Pyronin Y/Hoechst staining, and results analyzed using the LSRFortessa flow cytometer.

BrdU Incorporation

For BrdU incorporation assay, BrdU (100 mg/kg body weight; BD Biosciences) was injected intraperitoneally into mice for 12 hr before analysis. BrdU incorporation was determined by flow cytometric analysis using the BrdU Flow Kit (BD Biosciences) according to the manufacturer's instructions.

Homing Assay

Bone marrow cells (2×10^7) from either WT or $ICAM-1^{-/-}$ mice were labeled with carboxyfluorescein succinimidyl ester (CFSE) and used as donor cells for the homing assay (Cancelas et al., 2005). The proportions of HSPCs before (R1) and after (R2) transplantation were analyzed by flow cytometry. The homing index was calculated based on the ratio of R2 to R1.

Statistical Analysis

Data were analyzed with GraphPad Prism 5.0 software (La Jolla, CA). Results were expressed as mean ± SEM and analyzed with the Student t test, Wilcoxon test, and one- or two-way ANOVA, as appropriate, followed by the relevant *post hoc* t test to determine p values. All data are derived from three to four independent experiments. The survival was analyzed using a log rank (Mantel-Cox) test.

Others experimental procedures are given in the Supplemental Information.

ACCESSION NUMBERS

The accession number for the RNA sequencing data reported in this report is GEO: GSE114836.

SUPPLEMENTAL INFORMATION

Supplemental Information includes Supplemental Experimental Procedures, seven figures, and five tables and can be found with this article online at https://doi.org/10.1016/j.stemcr.2018.05.016.

REFERENCES

Akashi, K., Traver, D., Miyamoto, T., and Weissman, I.L. (2000). A clonogenic common myeloid progenitor that gives rise to all myeloid lineages. Nature *404*, 193–197.

Arai, F., Hirao, A., Ohmura, M., Sato, H., Matsuoka, S., Takubo, K., Ito, K., Koh, G.Y., and Suda, T. (2004). Tie2/angiopoietin-1 signaling regulates hematopoietic stem cell quiescence in the bone marrow niche. Cell *118*, 149–161.

Beerman, I., Bhattacharya, D., Zandi, S., Sigvardsson, M., Weissman, I.L., Bryder, D., and Rossi, D.J. (2010). Functionally distinct hematopoietic stem cells modulate hematopoietic lineage potential during aging by a mechanism of clonal expansion. Proc. Natl. Acad. Sci. USA *107*, 5465–5470.

Blaser, B.W., Moore, J.L., Hagedorn, E.J., Li, B., Riquelme, R., Lichtig, A., Yang, S., Zhou, Y., Tamplin, O.J., Binder, V., et al. (2017). CXCR1 remodels the vascular niche to promote hematopoietic stem and progenitor cell engraftment. J. Exp. Med. *214*, 1011–1027.

Boyd, A.W., Wawryk, S.O., Burns, G.F., and Fecondo, J.V. (1988). Intercellular adhesion molecule 1 (ICAM-1) has a central role in cell-cell contact-mediated immune mechanisms. Proc. Natl. Acad. Sci. USA *85*, 3095–3099.

Bruns, I., Czibere, A., Fischer, J.C., Roels, F., Cadeddu, R.P., Buest, S., Bruennert, D., Huenerlituerkoglu, A.N., Stoecklein, N.H., Singh, R., et al. (2009). The hematopoietic stem cell in chronic phase CML is characterized by a transcriptional profile resembling normal myeloid progenitor cells and reflecting loss of quiescence. Leukemia *23*, 892–899.

Cancelas, J.A., Lee, A.W., Prabhakar, R., Stringer, K.F., Zheng, Y., and Williams, D.A. (2005). Rac GTPases differentially integrate signals regulating hematopoietic stem cell localization. Nat. Med. *11*, 886–891.

Carrasco, Y.R., Fleire, S.J., Cameron, T., Dustin, M.L., and Batista, F.D. (2004). LFA-1/ICAM-1 interaction lowers the threshold of B cell activation by facilitating B cell adhesion and synapse formation. Immunity *20*, 589–599.

Chambers, S.M., Shaw, C.A., Gatza, C., Fisk, C.J., Donehower, L.A., and Goodell, M.A. (2007). Aging hematopoietic stem cells decline in function and exhibit epigenetic dysregulation. PLoS Biol. *5*, e201.

Chen, S., Lewallen, M., and Xie, T. (2013). Adhesion in the stem cell niche: biological roles and regulation. Development *140*, 255–265.

Cheng, T., Rodrigues, N., Shen, H., Yang, Y., Dombkowski, D., Sykes, M., and Scadden, D.T. (2000). Hematopoietic stem cell quiescence maintained by p21cip1/waf1. Science *287*, 1804–1808.

Chitteti, B.R., Kobayashi, M., Cheng, Y., Zhang, H., Poteat, B.A., Broxmeyer, H.E., Pelus, L.M., Hanenberg, H., Zollman, A., Kamocka, M.M., et al. (2014). CD166 regulates human and murine hematopoietic stem cells and the hematopoietic niche. Blood *124*, 519–529.

Crane, G.M., Jeffery, E., and Morrison, S.J. (2017). Adult haematopoietic stem cell niches. Nat. Rev. Immunol. *17*, 573–590.

Doulatov, S., Notta, F., Laurenti, E., and Dick, J.E. (2012). Hematopoiesis: a human perspective. Cell Stem Cell *10*, 120–136.

Dykstra, B., Olthof, S., Schreuder, J., Ritsema, M., and de Haan, G. (2011). Clonal analysis reveals multiple functional defects of aged murine hematopoietic stem cells. J. Exp. Med. *208*, 2691–2703.

Ergen, A.V., Boles, N.C., and Goodell, M.A. (2012). Rantes/Ccl5 influences hematopoietic stem cell subtypes and causes myeloid skewing. Blood *119*, 2500–2509.

Geiger, H., Denkinger, M., and Schirmbeck, R. (2014). Hematopoietic stem cell aging. Curr. Opin. Immunol. *29*, 86–92.

Goncalves, K.A., Silberstein, L., Li, S., Severe, N., Hu, M.G., Yang, H., Scadden, D.T., and Hu, G.F. (2016). Angiogenin promotes hematopoietic regeneration by dichotomously regulating quiescence of stem and progenitor cells. Cell *166*, 894–906.

Greenbaum, A., Hsu, Y.M., Day, R.B., Schuettpelz, L.G., Christopher, M.J., Borgerding, J.N., Nagasawa, T., and Link, D.C. (2013). CXCL12 in early mesenchymal progenitors is required for haematopoietic stem-cell maintenance. Nature *495*, 227–230.

Itkin, T., and Lapidot, T. (2011). SDF-1 keeps HSC quiescent at home. Blood *117*, 373–374.

Jeannet, R., Cai, Q., Liu, H., Vu, H., and Kuo, Y.H. (2013). Alcam regulates long-term hematopoietic stem cell engraftment and self-renewal. Stem Cells *31*, 560–571.

Kent, D.G., Copley, M.R., Benz, C., Wohrer, S., Dykstra, B.J., Ma, E., Cheyne, J., Zhao, Y., Bowie, M.B., Zhao, Y., et al. (2009). Prospective isolation and molecular characterization of hematopoietic stem cells with durable self-renewal potential. Blood *113*, 6342–6350.

Liang, O.D., Lu, J., Nombela-Arrieta, C., Zhong, J., Zhao, L., Pivarnik, G., Mondal, S., Chai, L., Silberstein, L.E., and Luo, H.R. (2013). Deficiency of lipid phosphatase SHIP enables long-term reconstitution of hematopoietic inductive bone marrow microenvironment. Dev. Cell *25*, 333–349.

Long, E.O. (2011). ICAM-1: getting a grip on leukocyte adhesion. J. Immunol. *186*, 5021–5023.

Mendelson, A., and Frenette, P.S. (2014). Hematopoietic stem cell niche maintenance during homeostasis and regeneration. Nat. Med. *20*, 833–846.

Morita, Y., Ema, H., and Nakauchi, H. (2010). Heterogeneity and hierarchy within the most primitive hematopoietic stem cell compartment. J. Exp. Med. *207*, 1173–1182.

Nakamura-Ishizu, A., Takizawa, H., and Suda, T. (2014). The analysis, roles and regulation of quiescence in hematopoietic stem cells. Development *141*, 4656–4666.

Nilsson, S.K., Johnston, H.M., and Coverdale, J.A. (2001). Spatial localization of transplanted hemopoietic stem cells: inferences for the localization of stem cell niches. Blood *97*, 2293–2299.

Orford, K.W., and Scadden, D.T. (2008). Deconstructing stem cell self-renewal: genetic insights into cell-cycle regulation. Nat. Rev. Genet. *9*, 115–128.

Papayannopoulou, T., and Nakamoto, B. (1993). Peripheralization of hemopoietic progenitors in primates treated with anti-VLA4 integrin. Proc. Natl. Acad. Sci. USA *90*, 9374–9378.

Papayannopoulou, T., Craddock, C., Nakamoto, B., Priestley, G.V., and Wolf, N.S. (1995). The VLA4/VCAM-1 adhesion pathway

defines contrasting mechanisms of lodgement of transplanted murine hemopoietic progenitors between bone marrow and spleen. Proc. Natl. Acad. Sci. USA *92*, 9647–9651.

Peled, A., Kollet, O., Ponomaryov, T., Petit, I., Franitza, S., Grabovsky, V., Slav, M.M., Nagler, A., Lider, O., Alon, R., et al. (2000). The chemokine SDF-1 activates the integrins LFA-1, VLA-4, and VLA-5 on immature human CD34(+) cells: role in transendothelial/stromal migration and engraftment of NOD/SCID mice. Blood *95*, 3289–3296.

Pelletier, S.D., Hong, D.S., Hu, Y., Liu, Y., and Li, S. (2004). Lack of the adhesion molecules P-selectin and intercellular adhesion molecule-1 accelerate the development of BCR/ABL-induced chronic myeloid leukemia-like myeloproliferative disease in mice. Blood *104*, 2163–2171.

Pietras, E.M., Warr, M.R., and Passegue, E. (2011). Cell cycle regulation in hematopoietic stem cells. J. Cell Biol. *195*, 709–720.

Prosper, F., and Verfaillie, C.M. (2001). Regulation of hematopoiesis through adhesion receptors. J. Leukoc. Biol. *69*, 307–316.

Sawai, C.M., Babovic, S., Upadhaya, S., Knapp, D.J., Lavin, Y., Lau, C.M., Goloborodko, A., Feng, J., Fujisaki, J., Ding, L., et al. (2016). Hematopoietic stem cells are the major source of multilineage hematopoiesis in adult animals. Immunity *45*, 597–609.

Schepers, K., Hsiao, E.C., Garg, T., Scott, M.J., and Passegue, E. (2012). Activated Gs signaling in osteoblastic cells alters the hematopoietic stem cell niche in mice. Blood *120*, 3425–3435.

Schofield, R. (1978). The relationship between the spleen colony-forming cell and the haemopoietic stem cell. Blood Cells *4*, 7–25.

Scholer, A., Hugues, S., Boissonnas, A., Fetler, L., and Amigorena, S. (2008). Intercellular adhesion molecule-1-dependent stable interactions between T cells and dendritic cells determine CD8+ T cell memory. Immunity *28*, 258–270.

Simmons, P.J., Levesque, J.P., and Zannettino, A.C. (1997). Adhesion molecules in haemopoiesis. Baillieres Clin. Haematol. *10*, 485–505.

Suda, T., Arai, F., and Hirao, A. (2005). Hematopoietic stem cells and their niche. Trends Immunol. *26*, 426–433.

Suh, H.C., Ji, M., Gooya, J., Lee, M., Klarmann, K.D., and Keller, J.R. (2009). Cell-nonautonomous function of Id1 in the hematopoietic progenitor cell niche. Blood *114*, 1186–1195.

van de Stolpe, A., and van der Saag, P.T. (1996). Intercellular adhesion molecule-1. J. Mol. Med. (Berl.) *74*, 13–33.

Vermeulen, M., Le Pesteur, F., Gagnerault, M.C., Mary, J.Y., Sainteny, F., and Lepault, F. (1998). Role of adhesion molecules in the homing and mobilization of murine hematopoietic stem and progenitor cells. Blood *92*, 894–900.

Wilson, A., and Trumpp, A. (2006). Bone-marrow haematopoietic-stem-cell niches. Nat. Rev. Immunol. *6*, 93–106.

Wilson, A., Laurenti, E., Oser, G., van der Wath, R.C., Blanco-Bose, W., Jaworski, M., Offner, S., Dunant, C.F., Eshkind, L., Bockamp, E., et al. (2008). Hematopoietic stem cells reversibly switch from dormancy to self-renewal during homeostasis and repair. Cell *135*, 1118–1129.

Wilson, A., Laurenti, E., and Trumpp, A. (2009). Balancing dormant and self-renewing hematopoietic stem cells. Curr. Opin. Genet. Dev. *19*, 461–468.

Winkler, I.G., Barbier, V., Nowlan, B., Jacobsen, R.N., Forristal, C.E., Patton, J.T., Magnani, J.L., and Levesque, J.P. (2012). Vascular niche E-selectin regulates hematopoietic stem cell dormancy, self renewal and chemoresistance. Nat. Med. *18*, 1651–1657.

Xing, Z., Ryan, M.A., Daria, D., Nattamai, K.J., Van Zant, G., Wang, L., Zheng, Y., and Geiger, H. (2006). Increased hematopoietic stem cell mobilization in aged mice. Blood *108*, 2190–2197.

Zhang, C.C., Kaba, M., Ge, G., Xie, K., Tong, W., Hug, C., and Lodish, H.F. (2006). Angiopoietin-like proteins stimulate ex vivo expansion of hematopoietic stem cells. Nat. Med. *12*, 240–245.